Oxygen-Induced Vacancy Formation on a Metal Surface

M. Schmid, G. Leonardelli, M. Sporn, E. Platzgummer, W. Hebenstreit,* M. Pinczolits,† and P. Varga
Institut für Allgemeine Physik, TU Wien, Wiedner Hauptstrasse 8-10, A-1040, Austria
(Received 10 June 1998)

Using scanning tunneling microscopy, low-energy ion scattering, and quantitative low-energy electron diffraction, we find about 17% metal vacancies on the oxygen-covered Cr(100) surface. The oxygen atoms occupy all the hollow sites of the first layer, including those neighboring a Cr vacancy. We argue that the vacancy formation is energetically favored and not caused by stress but by electronic effects. [S0031-9007(98)08211-8]

PACS numbers: 68.35.Bs, 68.35.Dv, 82.65.My

Because of the high vacancy formation energy [1], the existence of isolated vacancies on metal surfaces is usually restricted to conditions far from thermodynamic equilibrium (e.g., sputtering at low temperatures). The only thermodynamically stable arrangements of vacancies at metal surfaces known so far are vacancies clustered to rows or other structures, such as in the missing row reconstructions of fcc(110) surfaces. In the present Letter, we report on oxygen-induced formation of *isolated* metal vacancies on the Cr(100) surface. This "atomic-scale pitting" is in sharp contrast to the macroscopic oxidation behavior of Cr, which gains its exceptional corrosion resistance from a smooth protective oxide layer.

All measurements were performed at room temperature in UHV with a base pressure below 10^{-10} mbar; with one UHV system for scanning tunneling microscopy (STM) and low-energy ion scattering (LEIS) and a separate UHV system with a mu metal chamber for quantitative low-energy electron diffraction (LEED). Auger electron spectroscopy (AES) was used in both UHV systems to ensure that the sample composition was the same for STM/LEIS and LEED. STM constant current topographs were obtained with negative sample bias, using an electrochemically etched *W* tip. The procedure for acquisition of LEED spot intensities is the same as described in Ref. [2], the experimental data used are seven nonequivalent beams with a total energy range of approximately 1550 eV. For the LEED calculations we have used the van Hove subroutines [3]. We have used the average t-matrix (ATA) approximation [4] to account for layers not fully occupied by one species (i.e., mixing the t matrices of the atom and of a vacancy, the latter being zero), an approach already successfully used for nonstoichiometric carbides [5]. An automated search algorithm [6] based on the tensor LEED approximation [7] was used to find the best-fit structure minimizing the Pendry R-factor. Error estimates are based on the variance of R_P [8] and include the effects of coupling of all parameters, including the Debye temperatures of O and the first Cr layer.

The results were obtained on a Cr(100) single crystal. Upon annealing, bulk impurities, such as C, O, and N segregate to the surface. Choosing appropriate preparation conditions, it is possible to prepare a surface covered almost exclusively with one segregant [9], which is oxygen after N depletion and annealing to temperatures near 900 °C. AES indicates that O reaches its saturation coverage at 900 °C, this coverage is about one monolayer. STM images (Fig. 1a) of this surface show "holes," i.e., depressions appearing about 50 pm deep. The holes make up for approximately 17% of all lattice sites; in all other equivalent lattice sites protrusions are visible. The holes show only some short range ordering, in a few places forming a $(\sqrt{5} \times \sqrt{5})R27°$ superstructure; the order is too weak to result in well-defined peaks in either the Fourier transform of the STM image or the LEED pattern. Annealing at lower temperature leads to less oxygen (as measured by AES) and fewer holes, and shows that such holes appear only at oxygen concentrations above a threshold of approximately $1/3$ of the saturation coverage. While oxygen atoms are usually imaged as depressions (holes) in STM, we do not expect to find oxygen in what one usually considers metal positions. As the number of holes observed is significantly lower than the oxygen coverage, the interpretation of the holes as oxygen positions is unlikely.

In previous work, we have shown that the pure Cr(100) surface is imaged by STM with inverse corrugation (atoms appear as depressions) [2,9]. If we had inverse corrugation also on the oxygen-covered surface, the holes would be in fourfold hollow sites. Inverse corrugation was attributed to the surface state of Cr(100) near the Fermi level [10]. The $p(1 \times 1)$ N/Cr(100) surface, which does not show this surface state, is imaged with regular corrugation (Cr atoms appear as protrusions) [2]. STM spectroscopy does not show this surface state on the O-covered surface either, indicating regular corrugation there. The holes should therefore reside in Cr sites.

This is confirmed by images showing both O-induced holes and the $c(2 \times 2)$ nitrogen superstructure (Fig. 1b). As the N atoms are known to reside in fourfold hollow sites [2], the two lines in Fig. 1b pass over hollow and bridge sites, but between the holes. Therefore the holes in Figs. 1a and 1b are truly in the positions of Cr atoms.

STM images taken after *adsorption* of oxygen at room temperature (RT) on pure Cr(100) show that O atoms are

 © 1999 The American Physical Society

imaged as depressions (Fig. 2a). With increasing O dose, the density of these depressions increases and patches of a $p(1 \times 1)$ superstructure form. In these patches, we find the same kind of holes as described above (Fig. 2b). As the holes mark lattice positions of Cr atoms, the images show that O resides in fourfold hollow sites as one would expect for such a surface.

Low-energy ion scattering with 1 keV He^+ ions, 90° scattering angle and incidence angles ψ below 30° (with respect to the surface plane) on Cr(100) with either segregated or adsorbed oxygen shows an oxygen signal stronger in [001] azimuth than in [011]. This confirms oxygen in fourfold hollow sites.

As a first test whether the holes could be vacancies, we performed incidence-angle dependent ion scattering (impact collision ion scattering spectroscopy, ICISS) [11]. On pure Cr(100), ICISS with 5 keV Ne^+ shows a sharp rise of the count rate at the critical angle of $\psi_c = 16°$, where the nearest neighbor Cr atoms emerge from the shadow cone (Fig. 3). With saturation coverage of segregated oxygen, we find a shoulder in the range of the critical angle expected for the double Cr-Cr distance ($\psi_c = 10°$). This result is in agreement to Cr vacancies on the surface. It should be noted, however, that the ICISS data alone could be also interpreted in other ways, e.g., assuming a large buckling of the first layer.

For a confirmation of the vacancy model, we have employed quantitative LEED. Without allowing for vacancies in the Cr lattice, but otherwise searching for the best fit between experiment and calculation, we get a Pendry R-factor of $R_P = 0.180$. Allowing for disordered vacancies in the Cr layer, and again minimizing all geometrical parameters results in 20% Cr vacancies and an improved $R_P = 0.154$, the resulting geometrical parameters are shown in Fig. 4(a). Given the accuracy expected for LEED and the fact that LEED and STM were done in separate UHV chambers, the agreement between the Cr vacancy concentrations derived by LEED and STM (17%) is excellent. The variance of R_P [8] is 0.024, indicating that a full occupation of the first Cr layer is slightly outside the error bars of the LEED

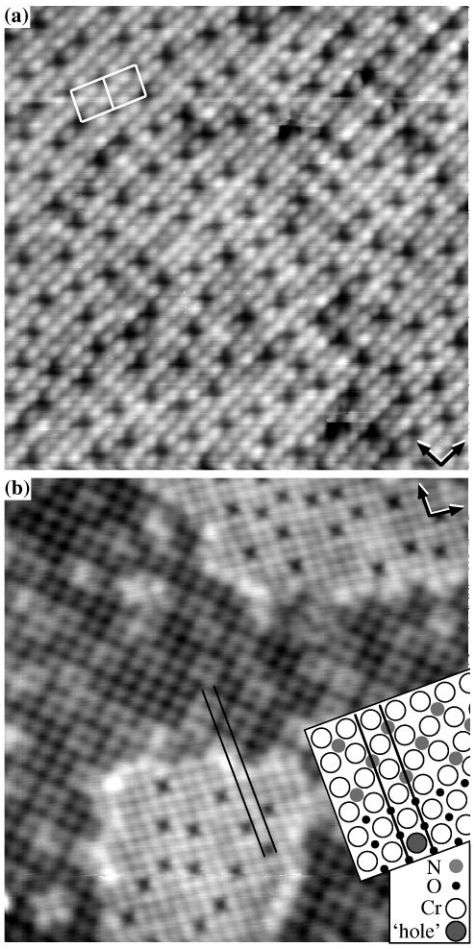

FIG. 1. STM images (10×10 nm^2) of the Cr(100) surface at (a) saturation coverage of segregated oxygen with two $(\sqrt{5} \times \sqrt{5})R27°$ cells marked and (b) domains of $c(2 \times 2)$ segregated N coexisting with saturated oxygen covered domains. Since N is known to reside in fourfold hollow positions [2], the two black lines show that the "holes" (vacancies) in the bright oxygen-covered areas are in Cr positions. N sites are probably imaged as depressions (dark), but the same result would be obtained with N appearing as protrusions. Arrows indicate the [001] and [010] directions. Tunneling voltage and current are (a) −0.19 V/8 nA and (b) −0.46 V/6 nA.

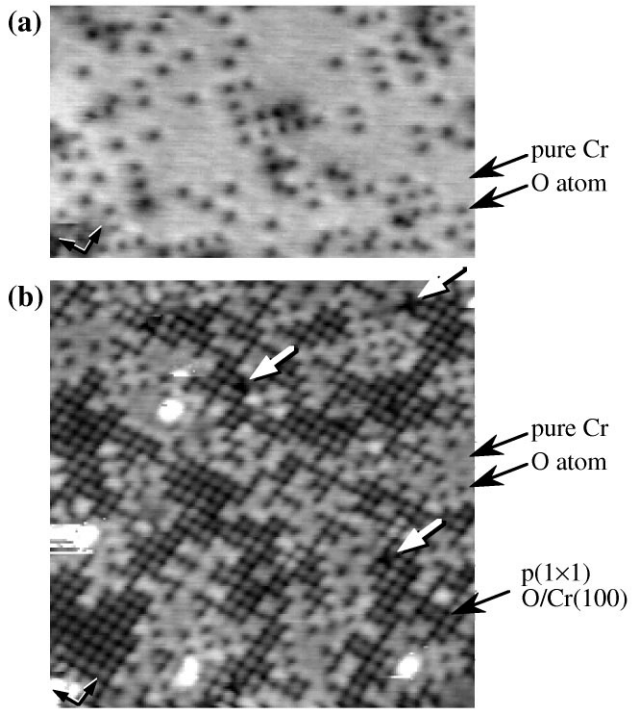

FIG. 2. STM images of the Cr(100) surface (10 nm wide) after adsorption of approximately (a) 0.7 L and (b) 2 L O_2 (1 L $= 1.33 \times 10^{-6}$ mbar s). White arrows point at "holes" (vacancies) appearing in the $p(1 \times 1)$ regions. The (anti-)-corrugation of the pure Cr areas is too weak to be visible (<5 pm). Tunneling parameters are (a) −0.5 mV/0.5 nA and (b) −0.5 mV/1.2 nA.

study. As we have the experience that the variance of R_P applied to ATA concentrations is a rather pessimistic error estimate [12], it is a strong confirmation of the existence of Cr vacancies. Allowing for partial occupation in the oxygen layer does not improve this result, indicating that all fourfold hollow sites, including these adjacent to a Cr vacancy, are occupied by oxygen. The R-factor in the present study is close to that obtained for $c(2 \times 2)$N on the same crystal ($R_P = 0.16$) [2], indicating that it is about the minimum achievable with the given setup and crystal. The low R-factor also rules out structural models deviating significantly from the one presented here, e.g., subsurface oxygen.

We have also performed a fit of the LEED data with a $(\sqrt{5} \times \sqrt{5})R27°$ structure model (Fig. 4b), which has exactly the same Cr vacancy concentration as the best-fit ATA result (20%). Only integer beams have been used. This results in an R-factor of $R_P = 0.161$, reflecting the fact that the structure is actually not well ordered. Nevertheless, further confirmation of the vacancy model comes from the calculated $(1/5, 2/5)$ and $(1/5, 3/5)$ superstructure spots showing pronounced maxima at 112 and 206 eV, in good agreement to the only energies where we have seen very weak and fuzzy $(\sqrt{5} \times \sqrt{5})R27°$ superstructure peaks on the LEED screen (108 and 204 eV). Further results of this model are a buckling in the O layer and the first Cr layer; but these values have very large error bars about the same size as the respective buckling amplitudes. The in-plane motions x_1 and y_1 of the Cr atoms surrounding a vacancy (Fig. 4b) are almost zero. As the actual structure shows only *local* $(\sqrt{5} \times \sqrt{5})R27°$ order, so we could not use any superstructure beams for the fit, the latter result stems only from multiple scattering events. Therefore, the R-factor does not depend sensitively on the in-plane coordinates of the Cr atoms. Nevertheless, the error bars are sufficiently small to show the absence of large in-plane motions of the Cr atoms (Fig. 4b). Since the LEED data are not sufficiently sensitive to the in-plane coordinates of the O atoms, these positions are assumed to form a regular square lattice.

Having established the existence of Cr vacancies, we have to find out the driving force of reconstruction, i.e., why the vacancies are formed. As neither pure nor N-covered Cr(100) nor any other unreconstructed metal surface studied by us so far shows any signs of metal vacancies, the formation of isolated Cr vacancies is a specific property of the O/Cr(100) surface. The vacancies form at both room temperature and at elevated temperature, and therefore cannot be due to kinetic limitations. This rules out vacancy formation by removal of Cr atoms for the creation of oxide islands (only found at room temperature) or sublimation of Cr at 900 °C. The structure is not sensitive to the cooldown rate, also indicating that we study the thermodynamic equilibrium configuration frozen in at some temperature between 900 °C and RT. Given the pronounced short-range order of the vacancies, we also do not believe entropy to play a major role. Therefore, the vacancies must be favored energetically.

One possible reason for vacancy formation could be compressive surface stress caused by the additional space required for the oxygen atoms. The O atoms occupy positions almost coplanar with the first-layer Cr atoms, nevertheless, the fourfold hollow sites of the bcc lattice offer much space for the O atoms. The sum of covalent

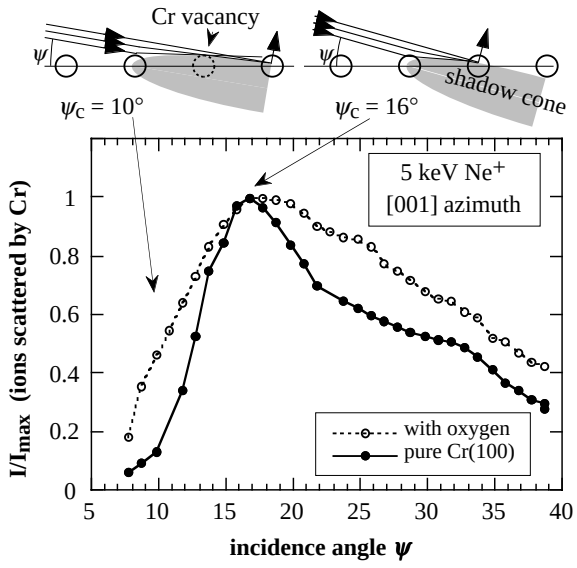

FIG. 3. Incidence angle dependent ion scattering signal from the pure and oxygen-covered Cr(100) surfaces. The geometry at 10° and 16° incidence is shown above. The scattering angle was 90°.

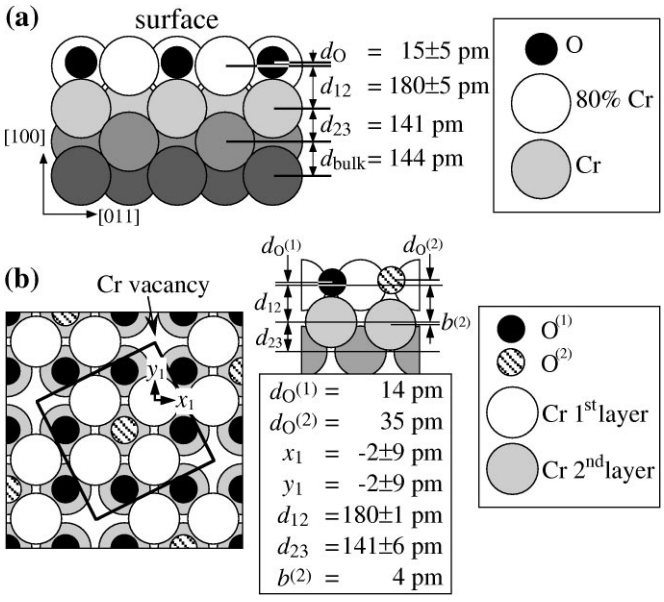

FIG. 4. Structure models employed in the LEED analysis together with the best-fit results for the parameters, assuming (a) disordered vacancies and (b) $(\sqrt{5} \times \sqrt{5})R27°$ ordered vacancies (corners of the square unit cell).

Cr and O radii is 191 pm, the sum of ionic O^{2-} and Cr^{2+} radii approximately 215 pm. As we do not assume the system to be fully ionic, the actual Cr-O distance of 205 pm should be enough to accommodate the O atoms. A further argument against compressive stress is the absence of large motion of the Cr atoms towards the vacancies.

Whereas structures like $p(1 \times 1)$ N/Cr(100) [13] and $p(1 \times 1)$ C/MoRe(100) [14] have been successfully related to bulk compounds with NaCl crystal structure like CrN and MoC, no such chromium oxide was found [15]. The large outward relaxation of the first Cr layer and the adsorbate positions are very similar to the $p(1 \times 1)$ N/Cr(100) structure [13], however. Comparison with NaCl-type oxides and nitrides of the elements neighboring Cr in the periodic table (Ti, V) can be used to estimate that a hypothetical NaCl type CrO should have a lattice constant of approximately 408 pm, perfectly fitting the Cr(100) lattice ($\sqrt{2}a_{\mathrm{Cr}} = 408$ pm). This can be seen as another argument against compressive stress in the first layer of $p(1 \times 1)$ O/Cr(100), as it is structurally equivalent to a (100) monolayer of an NaCl type CrO.

The similarity of the first layer to NaCl type bulk structures points us to a mechanism for vacancy formation in bulk crystals [16]. Whereas bulk carbides tend to form carbon vacancies, oxides form vacancies in both sublattices. The nitrides fall somewhere in between. For NbX (X = C, N, O) this fact was explained as a consequence of increased filling of nonbonding states with an increasing number of electrons in the X sublattice [16]. Cr contributes one more d-electron than Nb to the valance band formed from the nonmetal-p and metal-d electrons. Therefore, this effect should be more pronounced in NaCl-type Cr compounds. The surface structures obviously follow the same trend, as Cr vacancies are present only in the oxygen-covered Cr(100) surface, but not in $p(1 \times 1)$ N/Cr(100) [9]. We therefore suggest that similar electronic effects as in the bulk are responsible for the formation of Cr vacancies in the $p(1 \times 1)$ O/Cr(100) structure and possibly also the nonexistence of an NaCl type bulk CrO.

To conclude, on the Cr(100) surface covered with one monolayer oxygen we observe a chromium vacancy concentration of about 17% in the first monolayer. The existence of Cr vacancies was shown by STM, low-energy ion scattering and quantitative LEED. Cr vacancies were obtained after both room temperature adsorption of O_2 and segregation of O at high temperature. Whereas neither the atomic radii nor the comparison with bulk structures or the in-plane relaxations of the Cr atoms point to compressive stress as a driving force of the vacancy formation, electronic effects similar to those in bulk NaCl-type transition metal compounds are suggested as a reason for the vacancy formation.

We would like to thank U. Diebold and R. Podloucky for helpful discussions and Professor K. Heinz and his group for supplying the LEED computer programs and their help implementing them. This work was supported by the *Fonds zur Förderung der Wissenschaftlichen Forschung* (START Program No. Y-75 and Project No. P10492).

*Present address: Department of Physics, Tulane University, New Orleans, LA 70118.
†Present address: Institut für Halbleiterphysik, Johannes-Kepler Universität Linz, A-4040 Linz, Austria.

[1] Typically, between 0.3 and > 1 eV, see, e.g., H. M. Polatoglou, M. Methfessel, and M. Scheffler, Phys. Rev. B **48**, 1877 (1993).
[2] M. Sporn *et al.*, Surf. Sci. **396**, 78 (1998).
[3] M. A. Van Hove and S. Y. Tong, *Surface Crystallography by LEED*, Springer Series in Chemical Physics 2 (Springer, Berlin, 1979).
[4] F. Jona *et al.*, Phys. Rev. Lett. **40**, 1466 (1978); Y. Gauthier, Y. Joly, R. Baudoing, and J. Rundgren, Phys. Rev. B **31**, 6216 (1985).
[5] J. Rundgren, Y. Gauthier, and L. I. Johansson, Surf. Sci. **389**, 251 (1997).
[6] M. Kottcke and K. Heinz, Surf. Sci. **376**, 352 (1997).
[7] P. J. Rous *et al.*, Phys. Rev. Lett. **57**, 2951 (1986); P. J. Rous, Prog. Surf. Sci. **39**, 3 (1992); R. Döll, M. Kottcke, and K. Heinz, Phys. Rev. B **48**, 1973 (1993).
[8] J. B. Pendry, J. Phys. C **13**, 937 (1980).
[9] M. Schmid, M. Pinczolits, W. Hebenstreit, and P. Varga, Surf. Sci. **377–379**, 1023 (1997).
[10] J. A. Stroscio *et al.*, Phys. Rev. Lett. **75**, 2960 (1995).
[11] H. Niehus, W. Heiland, and E. Taglauer, Surf. Sci. Rep. **17**, 213 (1993).
[12] M. Sporn *et al.*, Surf. Sci. **416**, 423 (1998).
[13] Y. Joly, Y. Gauthier, and R. Baudoing, Phys. Rev. B **40**, 10 119 (1989); Y. Joly, Phys. Rev. Lett. **68**, 950 (1992).
[14] M. Kottcke *et al.*, Surf. Sci. **352-354**, 592 (1996).
[15] W. J. Kramers and J. R. Smith, Trans. Br. Ceram. Soc. **56**, 590 (1957).
[16] H. Erschbauer, R. Podloucky, and A. Neckel, J. Phys. F **15**, L279 (1985).